

EFFECT OF AG SUBSTITUTION ON STRUCTURAL, MAGNETIC AND MAGNETOCALORIC PROPERTIES OF $\text{Pr}_{0.6}\text{Sr}_{0.4-x}\text{Ag}_x\text{MnO}_3$ MANGANITES

R. Thaljaoui^{1,2,3}, M. Pękala², J.-F. Fagnard², Ph. Vanderbemden²

1. SUPRATECS, Department of Electrical Engineering and Computer Science (B28), University of Liège, Belgium;

2. Department of Chemistry, University of Warsaw, Al. Zwirki i Wigury 101, 02-089, Poland;

3. Faculty of Physics, Warsaw University of Technology, Koszykowa 75, 00-662 Warsaw, Poland

ABSTRACT: A systematic investigation on the structural, magnetic and magnetocaloric properties of $\text{Pr}_{0.6}\text{Sr}_{0.4-x}\text{Ag}_x\text{MnO}_3$ ($x=0.05$ and 0.1) manganites was reported. Rietveld refinements of the X-ray diffraction patterns confirmed that all samples were single phase and crystallized in the orthorhombic structure *with Pnma* space group. Magnetic measurements in a magnetic applied field of 0.01 T revealed that the ferromagnetic-paramagnetic transition temperature T_c decreased from about 293 to 290 K with increasing silver content from $x=0.05$ to 0.1 . The reported magnetocaloric entropy change and relative cooling power for both samples were considerably remarkable with a ΔS_{max} value of 1.9 J/(kg·K) and maximum RCP values of 100 J/kg, under a magnetic field change ($\Delta\mu_0 H$) equal to 1.8 T. The analysis of the universal curves gave an evidence of a second order magnetic transition for the studied samples. The magnetic field influence on both the magnetic entropy change and the relative cooling power was also studied and discussed.

KEYWORDS: monovalent doped manganite; XRD; SEM; ZFC and FC curves; magnetocaloric effect; universal curves; relative cooling power; critical exponents

Foundation item: Project supported by the Polish Government and WBI (Belgium) in a Frame of Mutual Scientific Exchange

Visits between WBI and Polish Ministry under project with reference numbers 14794/PVB/BE.POL/AN/an/2016/28611 and Rhea 2015/245812

Perovskite manganites have attracted considerable attention in the scientific community due to their complex phase diagrams and their important properties such as colossal magnetoresistance (CMR) and magnetocaloric effect (MCE)^[1-5]. The interest to these materials is motivated by their potential applications in magneto-electronic technology and magnetocaloric cooling devices. Magnetocaloric effect (MCE) is a characteristic property of magnetic materials that can produce or absorb heat by the action of a magnetic field change ΔH ^[6]. The practical interest to MCE is mainly related with its possible use for magnetic refrigeration that can be a viable and competing technology for gas-compression re-frigeration^[7]. There are several potential materials for magnetic refrigeration near room temperature. Gadolinium (Gd) is one of them but its price hinders its use for large scale applications and motivates research for cheaper materials. Recent studies suggest that many rare earth based alloys and oxides are interesting candidates for magnetic refrigeration^[8-13]. In addition to those, promising results were found in perovskite manganites. As an example, a large MCE even larger than that of Gd for $\text{La}_{1-x}\text{Ca}_x\text{MnO}_3$ manganite was reported^[14,15]. A substantial research activity has been carried out worldwide to investigate new perovskite materials with significant magnetocaloric effect and large CMR near room temperature. In fact perovskite manganites possess various advantages such as their very small magnetic hysteresis, high chemical stability, low cost, and high electrical resistivity which is beneficial to reducing the eddy-current heating. They can be easily manufactured using

various processes. Magnetic properties of manganites with general formula $RE_{1-x}T_xMnO_3$ where RE is a trivalent rare-earth and T is an alkaline or alkaline earth, are mainly related to the coexistence of a mixed-valent state $Mn^{3+}\text{-}Mn^{4+}$ which leads to ferromagnetic (FM) and anti-ferromagnetic (AFM) interaction originating from $Mn^{3+}\text{-}Mn^{4+}$, $Mn^{3+}\text{-}Mn^{3+}$ and $Mn^{4+}\text{-}Mn^{4+}$ ion pairs, respectively.

Moreover, the magnetic phases are strongly dependent on chemical composition, size of the grains, and mainly on the Mn^{4+}/Mn^{3+} ratio that can be easily affected by the substitution on the T-site. These parameters have a direct impact on their phase transition temperature and obviously on the CMR and MCE properties. It was reported that the CMR and MCE effects cannot be only explained by using double exchange mechanism (DE) without considering the Jahn-Teller effects, the cooperative ordering and the distortion of MnO_6 octahedron^[16]. Recent reports of $Pr_{1-x}Ag_xMnO_3$ system showed a reversal sign of MCE which was explained by the coexistence of the ferromagnetic and canted antiferromagnetic phases^[17], meanwhile the transition temperature $T_C=82.7$ K for $x=0.05$ is found to be far from room temperature, which limits their applicability in electronic and cooling devices. Perovskite manganites properties can be easily influenced by simple substitution in A-site or B-site as reported in literature^[18,19]. In our previous work we studied the effect of monovalent ions (Na^+ , K^+) in the Pr/Sr-site of $Pr_{0.6}Sr_{0.4}MnO_3$ system^[20-23]. The results confirmed a FM-PM phase transition near room temperature for all investigated samples, a large relative cooling power for the $Pr_{0.6}Sr_{0.4-x}Na_xMnO_3$ manganite^[20]. In addition, a significant MCE value was also observed for $Pr_{0.6}Sr_{0.4-x}K_xMnO_3$ and $Pr_{0.55}K_{0.05}Sr_{0.4}MnO_3$ compounds^[21,22]. Such results motivate to extend our previous studies on monovalent-doped manganites around room temperature. In the present work we reported the structural and magnetocaloric properties of $Pr_{0.6}Sr_{0.4-x}Ag_xMnO_3$ ($x=0.05$, and 0.1) samples. The exchange of the divalent Sr^{2+} with the larger monovalent Ag^+ increased the Mn^{4+}/Mn^{3+} ratio. This, in turn, enhances the mean ionic radius of A-site. In order to confirm the second order of the magnetic transition we reported the universal curves of magnetic entropy change. Magnetic field sensitivity of magnetic entropy change and relative cooling power were also analysed and discussed.

1 Experimental

Polycrystalline $Pr_{0.6}Sr_{0.4-x}Ag_xMnO_3$ ($x=0.05$ and 0.1) manganites were prepared by the conventional solid-state method. The starting elements Pr_6O_{11} , $SrCO_3$, Ag_2CO_3 and MnO_2 with the purity of 99.99% were preheated. The appropriate amounts of oxides were mixed in an agate mortar and then heated in air to 1000 °C for 60 h with intermediate grinding. The obtained mixtures were then pressed into pellets and sintered at 1100 °C in air for 60 h with intermediate grinding. Phase purity, homogeneity and cell parameters were checked by powder X-ray diffraction at room temperature with $Cu\ K\alpha$ radiation (0.154 nm) in the 2θ range of $10^\circ\text{-}100^\circ$. Structural analysis was carried out using the standard Rietveld technique^[24,25]. The morphology and grain size distribution were studied by using scanning electron microscopy (SEM). Magnetic measurements were carried out using a Quantum Design Physical Property Measurement System (PPMS). DC magnetization in zero field cooled (ZFC) and field cooled (FC) modes were recorded in a temperature range from 10 to 340 K under an applied field of 0.01 T. The isothermal magnetization ($M\text{-}H$) curves were recorded at different temperatures when the magnetic field was swept from 0 to 1.8 T.

2 Results and discussion

2.1 CRISTAL STRUCTURE AND MORPHOLOGY

Fig. 1 shows the XRD patterns of the $\text{Pr}_{0.6}\text{Sr}_{0.4-x}\text{Ag}_x\text{MnO}_3$ ($x=0.05$ and 0.1) samples. These patterns display a typical reflection with single-phase orthorhombic crystallographic structure. The diffraction data analysed by using the Rietveld powder diffraction profile fitting technique with space group $PNMA$ show a slight increase of the unit cell volume from 0.2307 to 0.2308 nm^3 for $x=0.05$ and 0.1 , respectively. Such volume increase can be explained with the increase of Ag^+ content with ionic radius 0.128 nm being larger than the ionic radius of Sr^{2+} (0.126 nm)^[26]. Similar results were reported previously for $\text{Pr}_{0.6}\text{Sr}_{0.4-x}\text{K}_x\text{MnO}_3$ manganites^[22]. The relation $b/\sqrt{2} < a < c$ is obeyed for both samples, which confirms the lattice deformation with the O' -structure is caused by the Jahn-Teller effect^[27]. The chemical composition of the samples was checked by the EDX technique and a typical plot is shown in Fig. 2 for the $x=0.1$ sample. EDX results confirm that monovalent elements did not evaporate during the preparation process. The SEM images shown in Fig. 3 confirm that both $\text{Pr}_{0.6}\text{Sr}_{0.4-x}\text{Ag}_x\text{MnO}_3$ materials are composed of irregular particles with grain size varying between 1 - 1.3 μm and 1.3 - 1.8 μm for $x=0.05$ and 0.1 , respectively. This result put into evidence that grains are larger than the values in the range 0.3 - 0.8 μm reported previously for the $\text{Pr}_{0.6}\text{Sr}_{0.4}\text{MnO}_3$ samples [20]. The larger grain size observed for silver doped materials indicates that Ag promotes particles coalescence as reported in Ref. [28].

Fig. 1 XRD patterns of $\text{Pr}_{0.6}\text{Sr}_{0.4-x}\text{Ag}_x\text{MnO}_3$ manganites with $x=0.05$ (a) and 0.1 (b), respectively

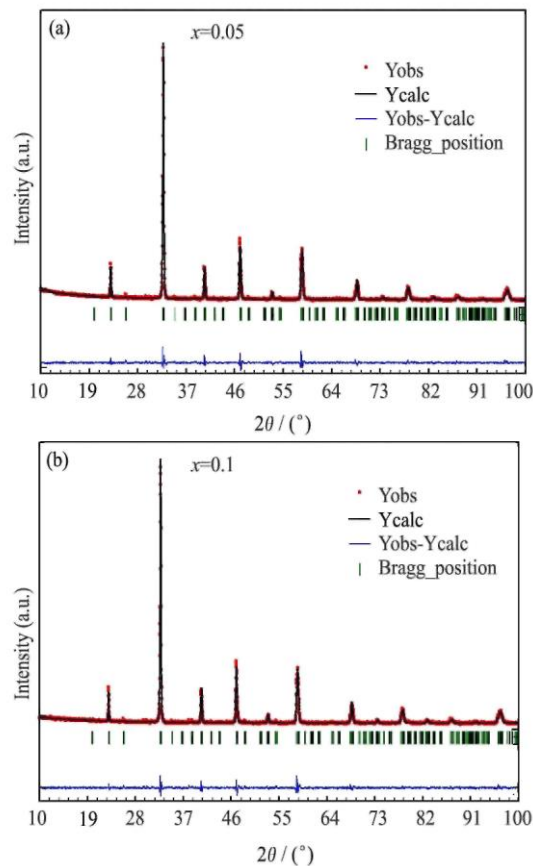


Fig. 2 EDX plot of $Pr_{0.6}Sr_{0.3}Ag_{0.1}MnO_3$ manganite

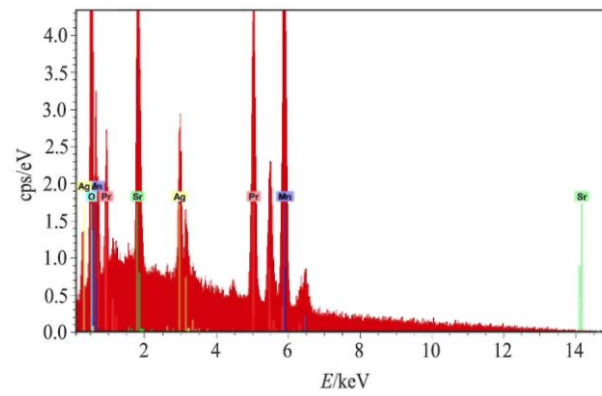


Fig. 3 Scanning electron micrograph for $Pr_{0.6}Sr_{0.4-x}K_xMnO_3$ manganites ($x=0.05$ (a) and 0.1 (b))

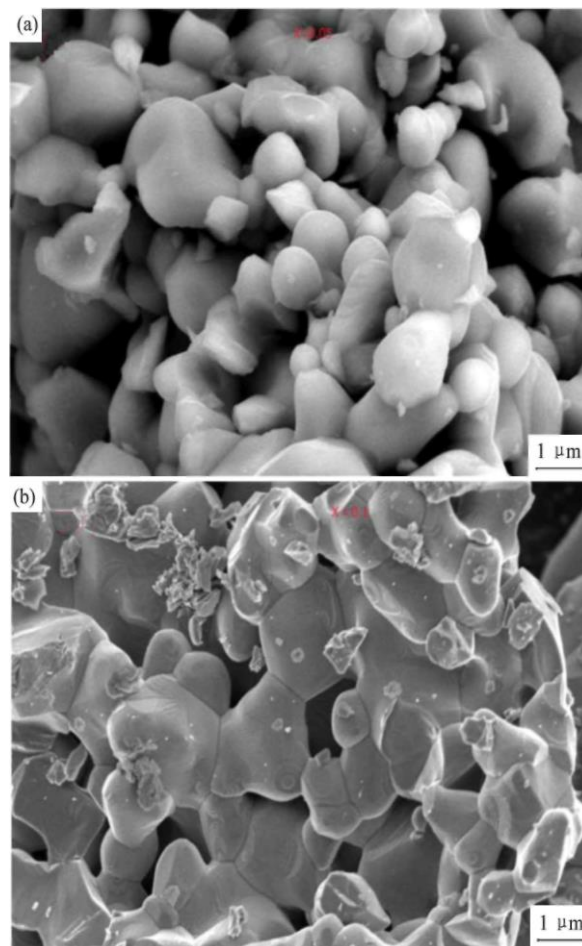
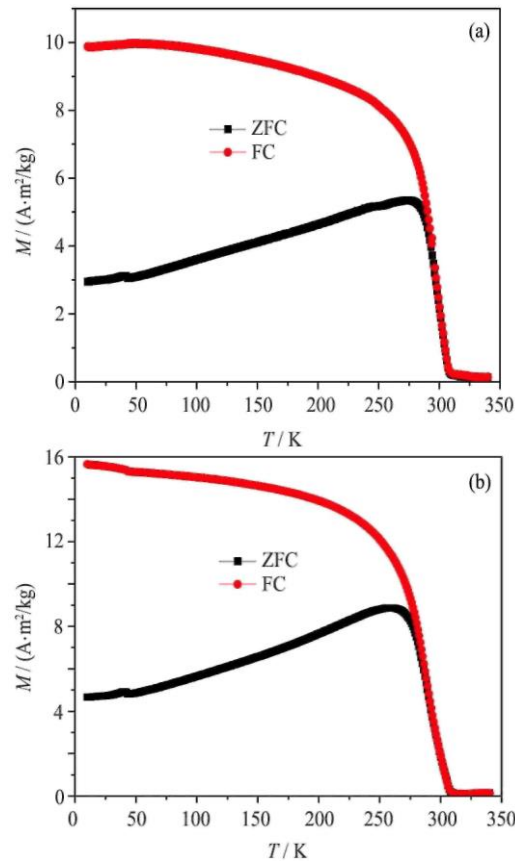


Fig. 4 Temperature variation of zero field cooled (ZFC) and field cooled (FC) measured at a magnetic field of 100 Oe for $\text{Pr}_{0.6}\text{Sr}_{0.4-x}\text{K}_x\text{MnO}_3$ manganites ($x=0.05$ (a) and 0.1 (b))



The mean crystallite size D was determined by using the width of XRD peaks according to Scherrer formula:

$$D = \frac{k\lambda}{\beta \cos\theta}$$

where D is the crystallite size (nm), k is the shape factor ($k=0.9$), λ is the wavelength of the X-rays ($k=0.154056$ nm for Cu $K\alpha$), β is the broadening of the diffraction peak measured at FWHM (in radians) and θ is the Bragg diffraction angle. The calculated values were found to vary between 37 and 44 nm. The crystallite sizes are significantly smaller than the grain sizes deduced from SEM micrographs, giving evidence that each grain consists of several crystallites.

2.2 MAGNETIC RESULTS

The temperature dependence of the magnetization of $\text{Pr}_{0.6}\text{Sr}_{0.4-x}\text{Ag}_x\text{MnO}_3$ ($x=0.05$ and 0.1) manganites during the cooling and warming mode was studied by carrying out measurements at low field (0.01 T) over a temperature range between 10 and 350 K. Both zero field cooled (ZFC) and field cooled (FC) modes are plotted in Fig. 4. For both materials, the magnetization is observed to sharply decrease in both ZFC and FC curves around the Curie temperature T_C which is related to the transition from the ferromagnetic to the paramagnetic state. Interestingly, a weak irregularity of ZFC and FC magnetization was observed at low temperature. Depending on the silver content, this corresponds to an abrupt magnetization change that has been explained by a structural transition from the high temperature orthorhombic $Pnma$ to the low temperature monoclinic I_2/a space group. Such a typical behaviour was reported previously for similar manganite materials^[20,29].

The inflexion point of the temperature derivative of magnetization was used to determine T_c values which are found to be 293 and 290 K for $x=0.05$ and 0.1 samples, respectively. The observed gradual decrease of T_c with increasing x content up to 0.1 is related to the effective weakening of the exchange interaction when the Mn^{3+} amount is reduced with increasing Ag content.

In order to further analyze the physical properties in relation to the structural results, we calculated the average bond angle of Mn-O-Mn and the average bond length of Mn-O, which in turn are used to determine the bandwidth W according to the following approximate formula:

$$W \propto \frac{\cos \frac{1}{2} (\Pi - \text{Mn} - \text{O} - \text{Mn})}{(d_{\text{Mn-O}})^{3.5}}$$

With increasing the x content from 0.05 to 0.1, the average bond angle of Mn-O-Mn slightly decreases from 161.1 to 161.06 degrees and the bond length of Mn-O increases from 0.1953 to 0.1955 nm. This results leads to the decrease of the bandwidth W from 0.0947 to 0.0944 for $x=0.05$ and 0.1 samples, respectively. Referring to the results plotted in Fig. 4, the ZFC and FC magnetization curves split below the irreversibility temperature T_{irr} which is here 284 and 276 K for $x=0.05$ and 0.1 samples, respectively. This irreversibility between ZFC and FC curves, as observed for similar doped manganites, suggests the presence of magnetic clusters^[30] and can also be explained by the magnetic inhomogeneity in the long range ferromagnetic-ordering^[31]. We should also note that on lowering temperature, the FC branch increases whereas a decreasing tendency is observed for the ZFC curve. As shown in Fig. 5, the magnetization variation between ZFC and FC curves ΔM versus temperature is observed to be the largest at 10 K and is found to decrease towards zero for $T > T_c$ with the biggest variation for $x=0.1$ sample. According to Fig. 5 the width of the irreversibility is dependent on the particles size mainly at low temperature ($T \ll T_c$) and is found to decrease with increasing particle size. A similar behaviour has been reported for $La_{0.6}Ca_{0.4}MnO_3$ manganite^[32].

In order to understand the nature of the PM-FM transition, the isothermal magnetization data have been recorded in a magnetic field change $\Delta \mu_0 H$ up to 1.8 T from 250 to 340 K for $x=0.05$ and from 241 to 340 K for $x=0.1$. The typical plot of the magnetization isotherms, shown in Fig. 6 for $x=0.05$ sample, indicates that magnetization M increases most abruptly in weak applied field ($\mu_0 H < 0.2$ T) and then approaches the saturation for $\mu_0 H > 1$ T. The saturated magnetization increases with decreasing temperature, suggesting a typical ferromagnetic behaviour of samples below the Curie temperature.

Fig. 5 Magnetization variation between ZFC and FC curves of ΔM versus temperature for $Pr_{0.6}Sr_{0.4-x}K_xMnO_3$ manganites ($x=0.05$ and 0.1)

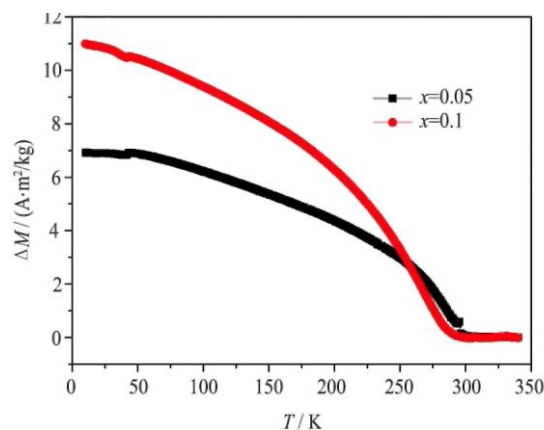
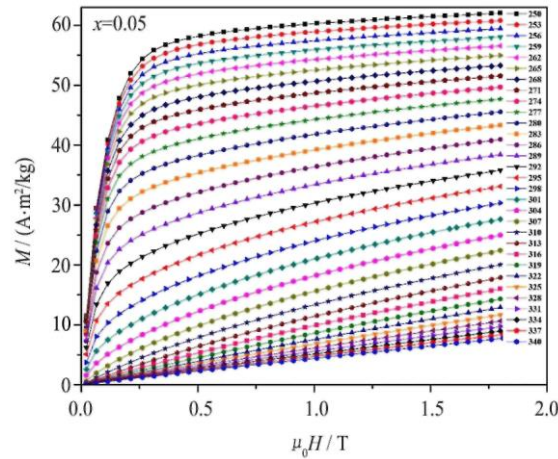


Fig. 6 Magnetization isotherms for $Pr_{0.6}Sr_{0.35}Ag_{0.1}MnO_3$ manganite



2.3 MAGNETIC ENTROPY

The magnetic entropy change ΔS , was calculated by using the isothermal magnetization measurements based on the thermodynamic Maxwell relation. The magnetic entropy change as a function of temperature at various magnetic fields is plotted in Fig. 7. All ΔS curves show similar shape and maximum values close to the phase transition temperature T_C . The maximum values of the entropy change in 0.05 silver doped manganites are found to be equal to 0.559, 1.12, 1.6 and 1.9 J/(kg·K) under $\Delta\mu_0H$ of 0.5, 1, 1.5 and 1.8 T, respectively. With increasing silver content to 0.1 the maximums of entropy change are slightly decreasing to be equal to 0.57, 1, 1.57 and 1.86 J/(kg·K) for $\Delta\mu_0H$ equal to 0.5, 1, 1.5 and 1.8 T. The maximum ΔS is observed in vicinity of room temperature for both silver doped samples and the width at a half maximum spreads up to about 54 K for a field variation equal to 1.8 T. Such results confirm that present compounds display very good properties for future cooling application near room temperature. We list in Table 1 the field change ($\Delta\mu_0H$), T_C , and ΔS_{\max} and values for our samples in comparison with other results reported in the literature^[20,21,33-35]. The ΔS_{\max} variation at phase transition temperature can be expressed by the following power relation^[36]:

$$|\Delta S_{\max}| \approx B^N \quad (3)$$

where $B=\mu_0H$ is the applied magnetic induction and N is a magnetic-ordering exponent. At T_C , the deduced N values from the best fit of $-\Delta S_{\max}(B)$ data from Fig. 8 according to Eq. (3) were found to be about 0.89 and 0.91 for $x=0.05$ and $x=0.1$, respectively. These values are close to $N=0.91$ observed for $La_{0.87}K_{0.13}MnO_3$ manganite^[37] and slightly higher than $N=0.72$ reported previously under considerably high applied field up to 7 T for un-doped $Pr_{0.6}Sr_{0.4}MnO_3$ manganite^[20]. Such difference can be explained easily by the dependence of maximum of the entropy change on magnetic field^[37]. The deviation from the value $N=2/3$ reported for mean field model in high field^[38] can be related to magnetic disorder and ferromagnetic cluster.

2.4 UNIVERSAL CURVES OF MAGNETIC ENTROPY CHANGE

The so-called universal curves of magnetic entropy change have been recently proposed by Franco et al.^[39,40] and successfully applied as a simple phenomenological method to construct universal entropy curves for various classes of materials. This approach was performed by normalizing the magnetic entropy change ΔS to its maximum value ΔS_{\max} for each magnetic field change. The temperature axis is transformed according to the following relation:

$$\begin{aligned} \theta &= -(T-T_C)/(T_{R1}-T_C) \text{ for } T < T_C \\ \theta &= (T-T_C)/(T_{R2}-T_C) \text{ for } T > T_C \end{aligned} \quad (4)$$

The so-called reference temperatures T_{R1} and T_{R2} correspond to the temperatures for which ΔS (T_{Ri})= $\Delta S_{max}/2$.

The typical plots for transformed $\Delta S/\Delta S_{max}(\theta)$ curves are shown in Fig. 9 for both studied manganites. This phenomenological method is considered to be one of the most accurate method to distinguish the nature of magnetic order. Generally magnetic order is deduced according to the Banerjee criterion stating that negative and positive slopes of H/M vs M^2 plots correspond to first order and second order transition, respectively^[41]. According to the method proposed by Franco et al, however, the nature of the magnetic order can be deduced from the field dependence of magnetic entropy change by using universal curves. Such a method suggests that if scaled curves measured under different applied magnetic fields follow an universal behaviour then it corresponds to a second order magnetic transition while if experimental data do not collapse in the same universal curve that is characteristic of a first order magnetic transition. In Fig. 8, a clear superposition into universal curves is observed for both samples. This behaviour is significantly different from that reported for $\text{La}_{0.66}\text{Y}_{0.04}\text{Ca}_{0.3}\text{MnO}_3$ manganite^[42] (first order phase transition). This indicates that the manganites studied undergo the second order magnetic phase transition.

Fig. 7 Temperature variation of magnetic entropy change at various magnetic field change for $\text{Pr}_{0.6}\text{Sr}_{0.4-x}\text{K}_x\text{MnO}_3$ manganites ($x=0.05$ (a) and 0.1 (b))

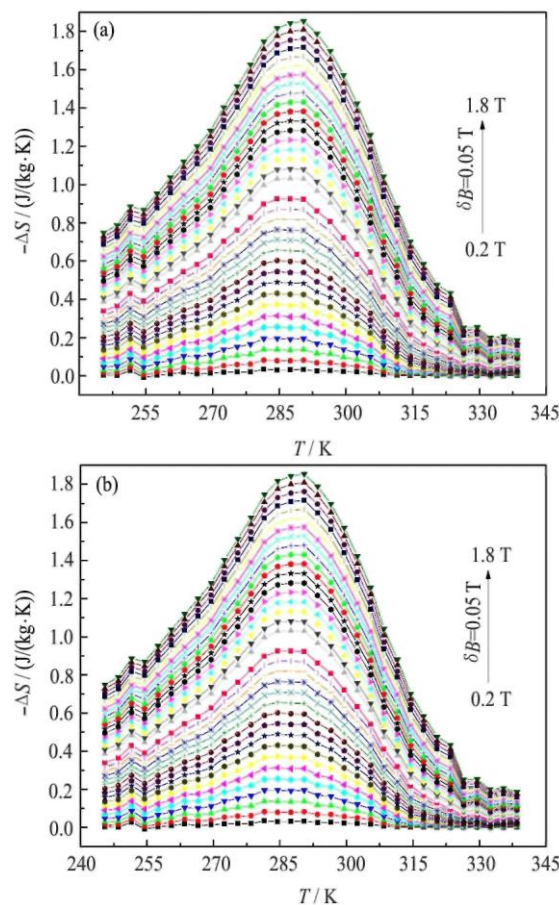
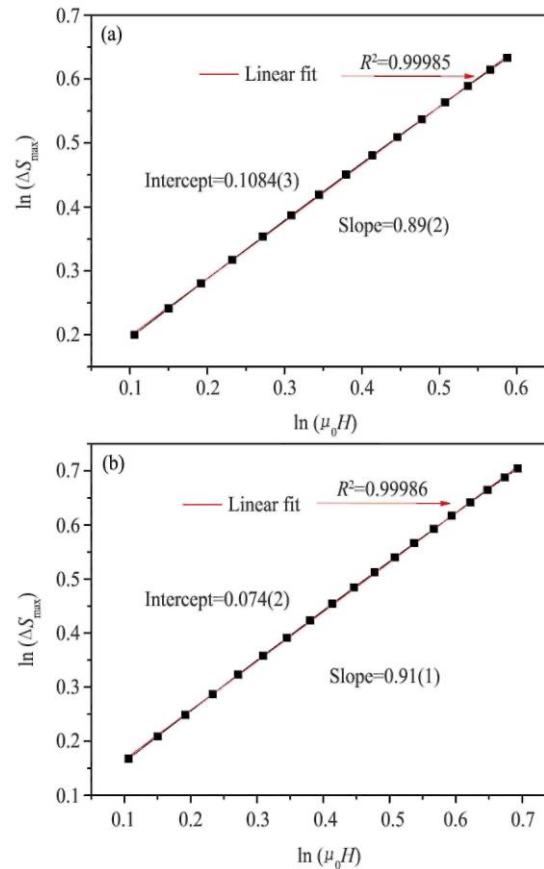


Fig. 8 Dependence of ΔS_{\max} at Curie temperature T_c on magnetic field for $\text{Pr}_{0.6}\text{Sr}_{0.4-x}\text{K}_x\text{MnO}_3$ manganites ($x=0.05$ (a) and 0.1 (b)) fitted according to Eq. (3)



2.5 COOLING POWER

Among other parameters used to assess the ability of material for magnetocaloric refrigeration, the so-called relative cooling power (RCP), describing an amount of heat transported between temperatures corresponding to the half maximum width δT_{FWHM} and the maximum entropy change ΔS_{\max} peak, was computed according to the following formula:

$$\text{RCP} = -\Delta S_{\max} * \delta T_{\text{FWHM}} \quad (5)$$

The RCP values calculated from our experimental data show that under an applied magnetic field change of 1.8 T the silver addition doping causes a slight increase of the RCP values from 93 to 100 J/kg for $x=0.05$ and 0.1 , respectively. This RCP increase can be related to the sample morphology and the extension of the interval δT which increases from 50 K for 0.05 sample to about 54 K for 0.1 sample under $\Delta \mu_0 H = 1.8$ T. We should also note that RCP values are comparable to those observed for $\text{Pr}_{0.6}\text{Sr}_{0.4-x}\text{Na}_x\text{MnO}_3$ and $\text{Pr}_{0.6}\text{Sr}_{0.4-x}\text{K}_x\text{MnO}_3$ manganites exhibiting the broader temperature half width as compared to present samples^[20,22]. We should note that with increasing silver content the RCP value is also increasing. Such behaviour can be related to the strong sensitivity of RCP to the microstructure created during various preparation and treatment steps.

The influence of magnetic field on RCP may be estimated according to the following formula^[41]: $\text{RCP}(B) \approx \text{const} (B)^R$ (6)

The R exponents values obtained from the numerical fit of RCP (Fig. 10) are found to be equal to 1.15 and 1.09 for $x=0.05$ and 0.1 , respectively. The deduced values are slightly higher than 1.04

reported previously for the undoped sample $\text{Pr}_{0.6}\text{Sr}_{0.4}\text{MnO}_3$ ^[17].

Fig. 9 Universal curves of magnetic entropy change for $\text{Pr}_{0.6}\text{Sr}_{0.4-x}\text{K}_x\text{MnO}_3$ manganites ($x=0.05$ (a) and 0.1 (b))

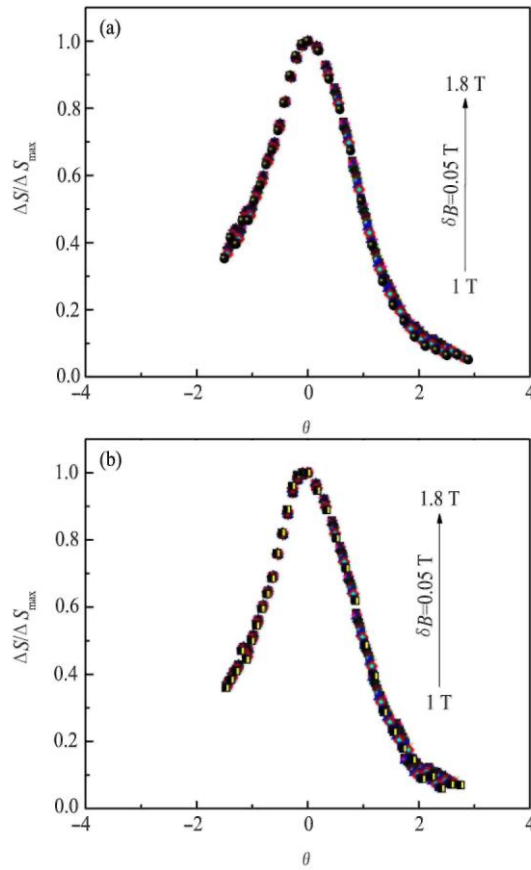
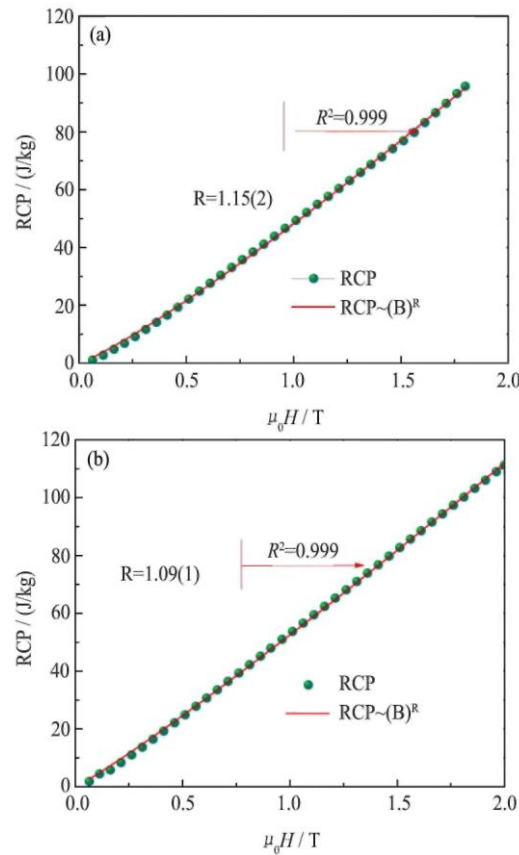


Fig. 10 Dependence of the RCP on magnetic field for $\text{Pr}_{0.6}\text{Sr}_{0.4-x}\text{K}_x\text{MnO}_3$ manganites ($x=0.05$ (a) and 0.1 (b)) fitted according to Eq. (6)



3 Conclusions

The investigation on the magnetocaloric properties of $\text{Pr}_{0.6}\text{Sr}_{0.4-x}\text{Ag}_x\text{MnO}_3$ ($x=0.05$ and 0.1) manganites revealed that the silver doping from 0.05 to 0.1 led to a slight shift of the Curie temperature T_C . Structural studies indicated that samples were single phase and characterized by an orthorhombic structure in the $Pnma$ space group. The analysis of magnetic data performed under a magnetic field change $\Delta\mu_0 H$ up to 1.8 T gave an evidence that the width of the irreversibility was strongly dependent on the particles size at low temperature ($T \ll T_C$). The second order nature of the magnetic transition was confirmed by the behaviour of the universal curves for both samples. The reported magnetocaloric results and the relative cooling power proved the potentiality of investigated samples for future cooling application near room temperature. The silver doping enhanced the dependence of the magnetic entropy change and relative cooling power in the range of investigated magnetic field changes ΔH . For a better understanding of the FM-PM transition nature, in the future work we will report in detail the critical exponents of studied samples in order to provide the nature of magnetic transition, the universality class, and the effective dimensionality of the phase transition around the Curie temperature T_C .

References:

- [1] Guo ZB, Du YW, Zhu J S, Huang H, Ding W P, Feng D. Large magnetic entropy change in perovskite-type manganese oxides. *Phys. Rev. Lett.*, 1997, 78: 1142.
- [2] Ramirez A P. Colossal magnetoresistance. *J. Phys.: Con-dens. Matter*, 1997, 9: 8171.
- [3] Millis A J, Shraiman B I, Mueller R. Dynamic Jahn-Teller effect and colossal magnetoresistance in $\text{La}_{1-x}\text{Sr}_x\text{MnO}_3$. *Phys. Rev. Lett.*, 1996, 77: 175.
- [4] Manosa L I, Planes A, Acet M, Manosa L I. Advanced materials for solid-state refrigeration. *J. Mater. Chem. A*, 2013,1: 4925.
- [5] Li L. Review of magnetic properties and magnetocaloric effect in the intermetallic compounds of rare earth with low boiling point metals. *Chin. Phys. B*, 2016,25: 037502.
- [6] Tishin A M. Handbook of Magnetic Materials, 1999,12.
- [7] Gschneidner Jr K A, Pecharsky V K, Tsokol A O. Recent developments in magnetocaloric materials. *Rep. Prog. Phys.*, 2005,68: 1479.
- [8] Li L W, Yuan Y, Zhang Y K, Namiki T, Nishimura K, Portgen R, Zhou S. Giant low field magnetocaloric effect and field-induced metamagnetic transition in TmZn . *Appl. Phys. Lett.*, 2015,107: 132401.
- [9] Li L W, Wang J, Su K P, Huo D X, Qi Y. Magnetic properties and magnetocaloric effect in metamagnetic $\text{RE}_2\text{Cu}_2\text{O}_5$ (RE=Dy and Ho) cuprates. *J. Alloys Compd.*, 2016,658:500.
- [10] Zhang Y K, Yang Y, Xu X, Hou L, Ren Z M, Li X, Wilde G. Large reversible magnetocaloric effect in $\text{RE}_2\text{Cu}_2\text{In}$ (RE= Er and Tm) and enhanced refrigerant capacity in its composite materials. *J. Phys. D: Appl. Phys.*, 2016, 49: 145002.
- [11] Li L, Niehaus O, Kersting M, Portgen R. Particle size dependence of the magnetic and magneto-caloric properties of HoCrO_3 . *Appl. Phys. Lett.*, 2014,104: 092416.
- [12] Zhang Y K, Yang B J, Wilde G. Magnetic properties and magnetocaloric effect in ternary REAgAl (RE=Er and Ho) intermetallic compounds. *J. Alloys Compd.*, 2015,12: 619.
- [13] Fujieda S, Fujita A, Fukamichi K. Large magnetocaloric effect in $\text{La}(\text{Fe}_x\text{Si}_{1-x})_{13}$ itinerant-electron metamagnetic compounds. *Appl. Phys. Lett.*, 2002, 81: 1276.
- [14] Guo Z B, Du Y W, Zhu J S, Huang H, Ding W P, Feng D. Bose-Einstein condensation of lithium: Observation of limited condensate number. *Phys. Rev. Lett.*, 1997, 78: 1142.
- [15] Phan M H, Yu S C. Review of the magnetocaloric effect in manganite materials. *J. Magn. Mater.*, 2007, 308: 325.
- [16] Millis A J, Littlewood P B, Shraiman B I. Double exchange alone does not explain the resistivity of $\text{La}_{1-x}\text{Sr}_x\text{MnO}_3$. *Phys. Rev. Lett.*, 1995, 74: 5144.
- [17] Gamzatov A G, Batdalov A B, Aliev A M, Khanov L N, Ahmadvand H, Salamati H, Kameli P. Magnetocaloric effect in $\text{Pr}_{1-x}\text{Ag}_x\text{MnO}_3$; manganites. *JETP Letters*, 2010, 91: 341.
- [18] Vadnala S, Pal P, Asthana S. Influence of A-site cation disorder on structural and magnetocaloric properties of $\text{Nd}_{0.7-x}\text{La}_x\text{Sr}_{0.3}\text{MnO}_3$ ($x=0.0, 0.1, 0.2$ & 0.3). *J. Rare Earths*, 2015,33: 1072.
- [19] Chavez-Guerrero L, Medina-Lott B, Cienfuegos R F, Garza-Navarro M A, Vannier R N, Ringuédé A, Hinojosa M, Cassir M. Synthesis and characterization of $\text{LaNi}_x\text{Co}_{1-x}\text{O}_3$ Role of microstructure on magnetic properties. *J. Rare Earths*, 2015,33:277.

- [20] Thaljaoui R, Boujelben W, Pekala M, Pekala K, Cheikhrouhou-Koubaa W, Cheikhrouhou A. Magnetocaloric study of monovalent-doped manganites $\text{Pr}_{0.6}\text{Sr}_{0.4-x}\text{Na}_x\text{MnO}_3$ ($x=0-0.2$). *J. Mater. Sci.*, 2013, 48: 3894.
- [21] Thaljaoui R, Boujelben W, Pekala M, Pekala K, Fagnard J F, Vanderbemden P, Donten M, Cheikhrouhou A. Magnetocaloric effect of monovalent K doped manganites $\text{Pr}_{0.6}\text{Sr}_{0.4-x}\text{K}_x\text{MnO}_3$ ($x=0$ to 0.2). *J. Magn. Magn. Mater.*, 2014, 352: 6.
- [22] Thaljaoui R, Boujelben W, Pekala M, Pekala K, Antonowicz J, Fagnard J F, Vanderbemden P, Dabrowska S, Mucha J. Structural, magnetic and magneto-transport properties of monovalent doped manganite $\text{Pr}_{0.55}\text{K}_{0.05}\text{Sr}_{0.4}\text{MnO}_3$. *J. Alloys Compd.*, 2014, 611: 427.
- [23] Thaljaoui R, Boujelben W, Pekala M, Pekala K, Mucha J, Cheikhrouhou A. Structural, magnetic and transport study of monovalent Na-doped manganite $\text{Pr}_{0.55}\text{Na}_{0.05}\text{Sr}_{0.4}\text{MnO}_3$. *J. Alloys Compd.*, 2013, 558: 236.
- [24] Rietveld H M. A profile refinement method for nuclear and magnetic structures *J. Appl. Cryst.*, 1969,2: 65.
- [25] Roisnel T, Rodriguez-Carvajal J. Computer program FULLPROF, LLB-LCSIM. May 2003.
- [26] Shanon R D. Revised effective ionic radii and systematic studies of interatomic distances in halides and chalcogenides. *Acta Cryst. A*, 1976,32: 751.
- [27] Knizek K, Jiráček Z, Pollert E, Zounova F, Vratislav S. Structure and magnetic properties of $\text{Pr}_{1-x}\text{Sr}_x\text{MnO}_3$ perovskites. *J. Solid State Chem.*, 1992,100: 292.
- [28] Choithrani R, Bhat M A, Gaur N K. Influence of silver doping on the magnetoresistance and temperature coefficient of resistance in $\text{Pr}_{0.67}\text{Sr}_{0.33}\text{MnO}_3$. *J. Magn. Magn. Mater.*, 2014, 361: 19.
- [29] Roessler S, Nair Harikrishnan S, Roessler U K, Kumar C M N, Suja Elizabeth, Wirth S. Ferromagnetic transition and specific heat of $\text{Pr}_{0.6}\text{Sr}_{0.4}\text{MnO}_3$. *Phys. Rev. B*, 2011, 84: 184422.
- [30] Durta A, Gayathri N, Ranganathan R. Effect of particle size on the magnetic and transport properties of $\text{La}_{0.875}\text{Sr}_{0.125}\text{MnO}_3$. *Phys. Rev. B*, 2003, 68: 054432.
- [31] Daivajna M D, Ashok R, Okram G S. Electrical, thermal and magnetic studies on Bi-substituted LSMO manganites. *J. Magn. Magn. Mater.*, 2015,388: 90.
- [32] Andrade V M, Caraballo Vivas R J, Pedro S S, Tedesco J C G, Rossi A L, Coelho A A, Rocco D L, Reis M S. Magnetic and magnetocaloric properties of $\text{La}_{0.6}\text{Ca}_{0.4}\text{MnO}_3$ tunable by particle size and dimensionality. *Acta Mater.*, 2016,102:49.
- [33] Fan J Y, Pi L, Zhang L, Tong W, Ling L S, Hong B, Shi Y G, Zhang W C, Lu D, Zhang Y H. Magnetic and magnetocaloric properties of perovskite manganite $\text{Pr}_{0.55}\text{Sr}_{0.45}\text{MnO}_3$. *Physica B*, 2011, 406: 2289.
- [34] Gokhan Ünlü C, Emre Tanis Y, Burak Kaynar M, Simsek T, Ozcan S. Magnetocaloric effect in $\text{La}_{0.7}\text{Nd}_x\text{Ba}_{(0.3-x)}\text{MnO}_3$ ($x=0, 0.05, 0.1$) perovskite manganites. *J. Alloys Compd.*, 2017,704:58.
- [35] Xu L S, Chen L L, Fan J Y, Barner K, Zhang L, Zhu Y, Pi L, Zhang Y H, Shi D N. Room-temperature large magnetocaloric effect and critical behavior in $\text{La}_{0.6}\text{Dy}_{0.1}\text{Sr}_{0.3}\text{MnO}_3$. *Ceram. Int.*, 2016, 42: 8234.
- [36] Franco V, Blazquez J S, Ingale B, Conde A. The magnetocaloric effect and magnetic refrigeration near room temperature: materials and models. *Annu. Rev. Mater. Res.*, 2012,42:305.
- [37] Aliev A M, Gamzatov A G, Batdalov A B, Mankevich A S, Korsakov I E. Structure and magnetocaloric properties of $\text{La}_{1-x}\text{K}_x\text{MnO}_3$ manganites. *Physica B*, 2011,406: 885.
- [38] Oesterreicher H, Parker F T. Magnetic cooling near Curie temperatures above 300 K. *J. Appl. Phys.*, 1984, 55: 4334.

[39] Franco V, Blazquez J S, Conde A. Field dependence of the magnetocaloric effect in materials with a second order phase transition: A master curve for the magnetic entropy change. *Appl. Phys. Lett.*, 2006, 89: 222512.

[40] Bonilla C M, Herrero-Albillos J, Bartolome F, Garcia L M, Parra-Borderias M, Franco V. Universal behavior for magnetic entropy change in magnetocaloric materials: An analysis on the nature of phase transitions. *Phys. Rev. B*, 2010,81:224424.

[41] Banerjee B K. On a generalised approach to first and second order magnetic transitions. *J. Phys. Lett.*, 1964,12: 16.

[42] Phan T L, Ho T A, Manh T V, Dang N T, Jung C U, Lee B W, Thanh T D. Y-doped $\text{La}_{0.7}\text{Ca}_{0.3}\text{MnO}_3$ manganites exhibiting a large magnetocaloric effect and the crossover of first-order and second-order phase transitions. *J. Appl. Phys.*, 2015,118: 143902.